

*Biochimica et Biophysica Acta*, 601 (1980) 289–301

© Elsevier/North-Holland Biomedical Press

BBA 78929

## ON THE STRUCTURE OF THE HEMOCYANIN CHANNEL IN LIPID BILAYERS

T.J. McINTOSH<sup>a</sup>, J.D. ROBERTSON<sup>a</sup>, H.P. TING-BEALL<sup>a</sup>, A. WALTER<sup>b</sup> and G. ZAMPIGHI<sup>a</sup>

<sup>a</sup> *Department of Anatomy, Duke University Medical Center, Durham, NC 27710 and* <sup>b</sup> *Duke University Marine Laboratory, Beaufort, NC 28516 (U.S.A.)*

(Received March 5th, 1980)

*Key words: Hemocyanin; Conductance channel; Lipid bilayer; (Electron microscopy)*

### Summary

Keyhole limpet hemocyanin has been shown by others (Alvarez, O., Diaz, E. and Latorre, R. (1975) *Biochim. Biophys. Acta* 389, 444–448) to form single conductance channels in black lipid membranes. In an attempt to visualize how the large (300 Å) water-soluble hemocyanin molecule interacts with lipid bilayers, we have examined hemocyanin in the presence of lipids with the electron microscope. We find that incubation of lipids with keyhole limpet hemocyanin produces a characteristic 70 Å in diameter, ring-shaped particle or annulus associated with the bilayer. This annulus, which appears to be quite distinct from previously observed aggregated and dissociated forms of hemocyanin, may be responsible for the channel formation in black lipid membranes.

---

### Introduction

Hemocyanins are the oxygen-binding respiratory proteins that occur freely dissolved in the hemolymph of many invertebrates. The structure of hemocyanins from various arthropods and molluscs has been studied extensively by using electron microscopy [1–6]. The hemocyanins from several molluscs are cylindrical molecules, about 300 Å in diameter and 300–360 Å in length [2,4], with molecular weights of the order of  $9 \cdot 10^6$  [7]. It is now generally accepted that molluscan hemocyanins are built from 20 polypeptide chains, each consisting of eight covalently linked domains [5–7]. Molluscan hemocyanins are known to exist in a number of aggregation states depending on the conditions of the medium [5,8–11]. In particular, in 10 mM EDTA at pH

8.9, keyhole limpet hemocyanin completely dissociates into its subunits, which are 1/20 the size of the original molecule [11]. In *Helix pomatia* hemocyanin, Siezen and van Bruggen [5] have shown that this subunit appears as a flexible chain containing seven or eight irregularly shaped globules with diameters of 55–60 Å.

The hemocyanin from one mollusc, the keyhole limpet, interacts with bimolecular lipid membranes. Pant and Conran [12] have found that keyhole limpet hemocyanin decreases the electrical resistance of lipid membranes by as much as 6 orders of magnitude. Alvarez et al. [13] showed that the conductance increases occurred in discrete steps and suggested that hemocyanin conducts ions across the lipid bilayer through discrete channels. In later work, Latorre et al. [14] characterized the voltage-dependent nature of these channels.

Speculation on the molecular mechanisms of hemocyanin-induced ion transport through lipid bilayers has centered on the 300 Å hemocyanin molecule or the subunits obtained at high pH values [15,16]. However, as Ehrenstein and Lecar [17] have pointed out, the whole hemocyanin molecule is several times larger than the membrane thickness, and Blumenthal [15] has shown that the fragments induced by extensive dialysis at elevated pH do not form single channels. In the present study, we are interested in obtaining structural information on the state of association of hemocyanin in the presence of polar lipids.

## Materials and Methods

Keyhole limpet hemocyanin (99.5% pure) was purchased from Calbiochem, while lipids and alkane solvents were obtained from Sigma or Applied Science. Hemocyanins prepared from octopus, giant snail, whelk (*Busycon canaliculatum*), and land snail (*Helix pomatia*) were the kind gift of Dr. Joseph Bonaventura of the Duke University Marine Laboratory.

In this study, the hemocyanin molecule was interacted with lipids in three forms — monolayers, vesicles, and planar lipid membranes. Monolayers were formed from hexane solutions over water or 0.1 M KCl in a Kim-Ray surfactometer as previously described [18]. A solution of hemocyanin (usually 0.1 mg/ml in water or 0.1 M KCl, pH 7) was then injected under the monolayer. A carbon-coated copper electron-microscope grid was dipped down and up through the compressed monolayer and quickly negatively stained. Vesicles were prepared by drying a chloroform/lipid solution in a round-bottom flask and hydrating with a solution of hemocyanin. The lipid/hemocyanin/water solution was briefly mixed in a vortex mixer, allowed to equilibrate for times ranging from several minutes to several hours, pipetted onto an electron-microscope grid, and negatively stained. The interaction of hemocyanin with planar lipid films was studied by the use of uncoated electron-microscope grids or grids coated with a carbon film containing many small holes, the so-called 'holey grids' [19]. The bare grid or holey grid was suspended in a solution of 0.1 mg/ml hemocyanin in 0.1 M KCl. Lipid dissolved in decane was then spread on the grid either with a pipette or with a brush, much in the manner black lipid films are spread on a hole in a partition separating two

aqueous compartments [20]. The lipid/alkane solution was allowed to remain on the grid for a sufficient time for it to thin out over the holes in the grid, presumably to a single lipid bilayer with solvent. Before withdrawal of the grid from the solution, all excess lipid was removed from the surface of the solution by vacuum aspiration. The grid was then removed from the hemocyanin solution, rinsed with distilled water to wash away excess hemocyanin, and negatively stained. As a control, solutions of pure hemocyanin in solution were negatively stained in the absence of lipid.

The negative stains used in these experiments were 2% uranyl acetate in water and 1% neutralized sodium phosphotungstate. Electron microscopy was performed using a Philips 301 electron microscope equipped with an anticontamination device cooled with liquid  $N_2$ . An objective aperture of  $5 \cdot 10^{-3}$  rad was used and the state of focus of the micrographs was determined by optical diffraction of the bare carbon film close to the areas of interest. Tilting experiments were performed on selected grids using a Philips 400 electron microscope equipped with a goniometer stage which tilts  $\pm 30^\circ$ .

Bimolecular or black lipid membranes were formed according to the method of Mueller et al. [20] from a mixture of phospholipids and *n*-decane at a concentration of 12.5 mg phosphatidylserine or phosphatidylethanolamine per ml *n*-decane and 25 mg azolectin (soya bean lecithin) per ml *n*-decane. The lipid solution was spread with a brush or pasteur pipette across a hole of 3 mm diameter on a polyethylene or Teflon partition which separates two magnetically stirred aqueous chambers. Hemocyanin was added to either or both chambers after the membrane had thinned down to a black film. All the aqueous solutions were unbuffered 0.1 M KCl and all measurements were performed at room temperature (approx.  $22^\circ\text{C}$ ). Membrane conductance was determined using Ag/AgCl electrodes, a differential electrometer, a current-measuring operational amplifier (Analogue Device 48K), and a voltage generator. The current-voltage (*I-V*) curves were recorded 5 min after addition of hemocyanin. The membrane conductance was calculated from the slope of the linear region of the *I-V* curves between the range  $\pm 10$  mV.

## Results

Negatively stained solutions of pure keyhole limpet hemocyanin, with no lipid present, have a similar appearance to other gastropod hemocyanins [1–4]. In Fig. 1, two views of the cylindrical keyhole limpet hemocyanin molecule are seen. The side view gives a rectangular image, with both length and height being about 300 Å. Striations, the center-to-center spacing of which is about 60 Å, are present in this side view. The end-on view of the molecule is a circular image with outside diameter of 300 Å. The center of this circular image is occupied by a pool of stain about 90 Å in diameter. Two concentric electron-lucent circles surround this central pool of stain. The outer ring is usually continuous and approx. 30–35 Å thick. The inner ring is thinner and often discontinuous.

Figs. 2–4 show the results of the interaction of keyhole limpet hemocyanin with lipid monolayers, vesicles, and planar bilayers. Fig. 2A–C presents images of carbon-coated grids which have been dipped through monolayers of fatty

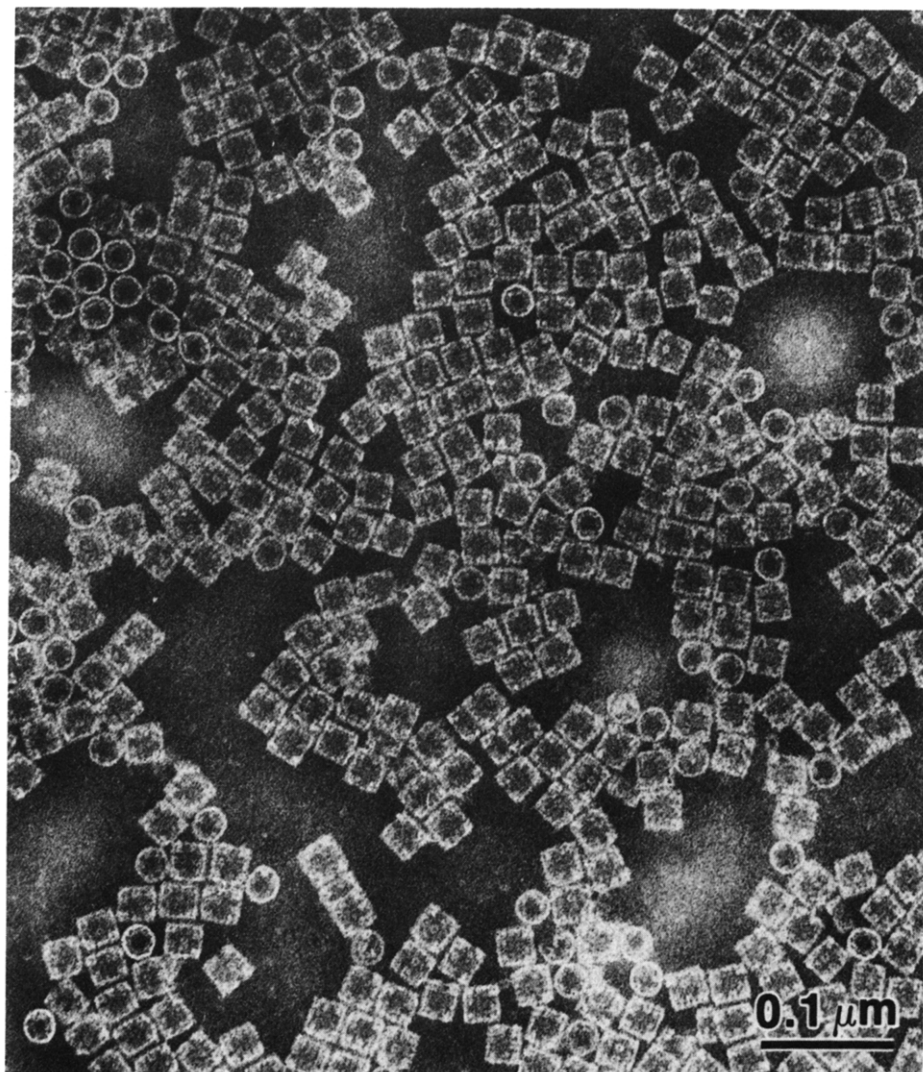


Fig. 1. Negatively stained preparation of pure keyhole limpet hemocyanin in water. The cylindrical hemocyanin molecule gives two images, a rectangular side view and a circular end-on view.

acid ( $\text{CH}_3(\text{CH}_2)_{20}\text{COOH}$ ) over a subsolution of hemocyanin. The transfer of fatty acid to epoxy and glass surfaces and carbon-coated electron-microscope grids has been extensively studied by both electron-microscopy and X-ray diffraction techniques [18,21–24]. The lipid monolayers are transferred to the substrate in bilayer form [24,25]. In Fig. 2A, the fatty acid has covered the entire microscope grid, giving a rather uniform, although mottled, appearance to the field. Scattered throughout the field are small (approx. 70 Å in diameter) circular-shaped objects. These particles have the appearance of rings or annuli, as stain invariably accumulates in their centers. The diameter of the stain in the center of each annulus is about 20 Å. This 70 Å annulus appears

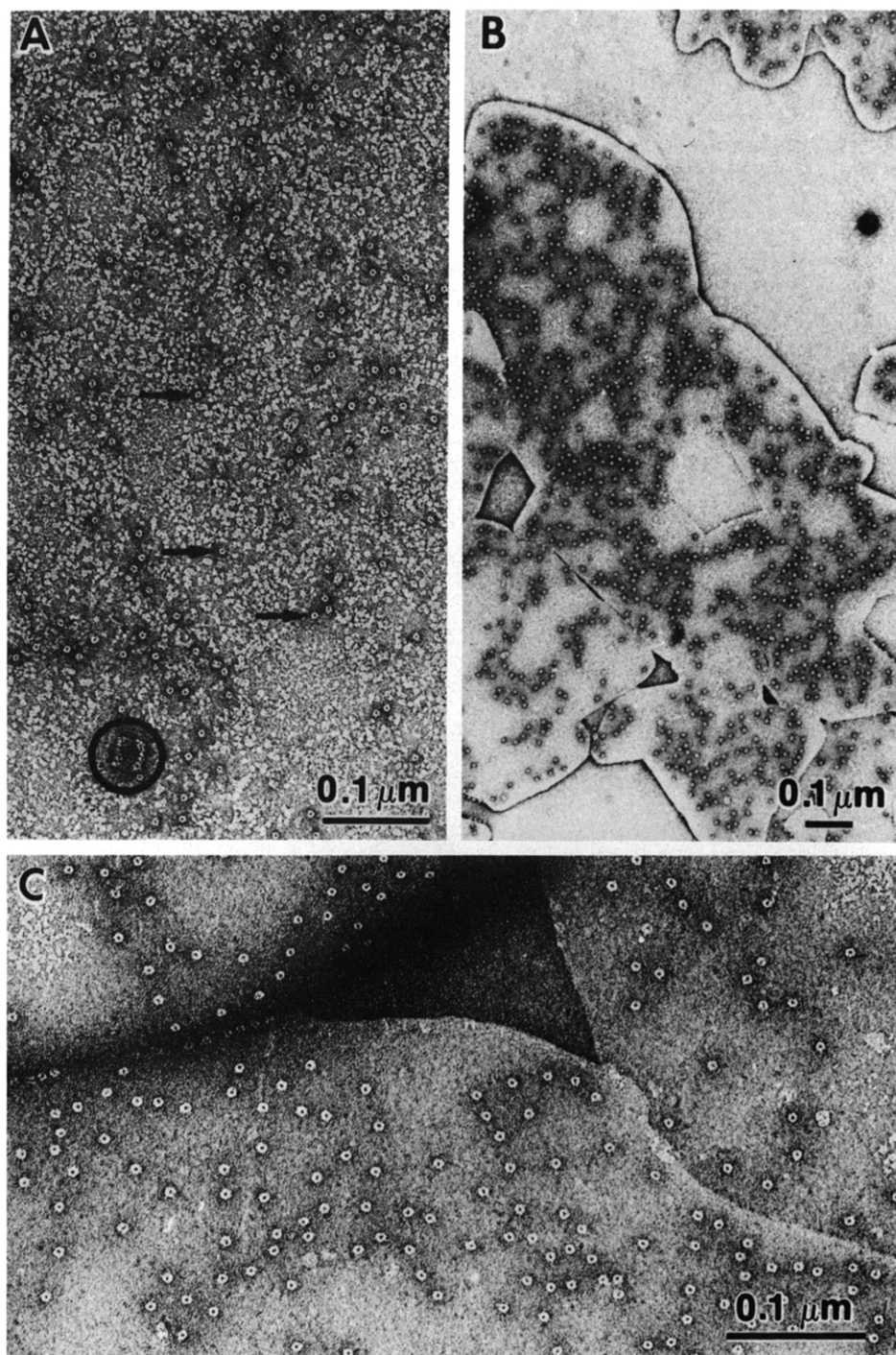
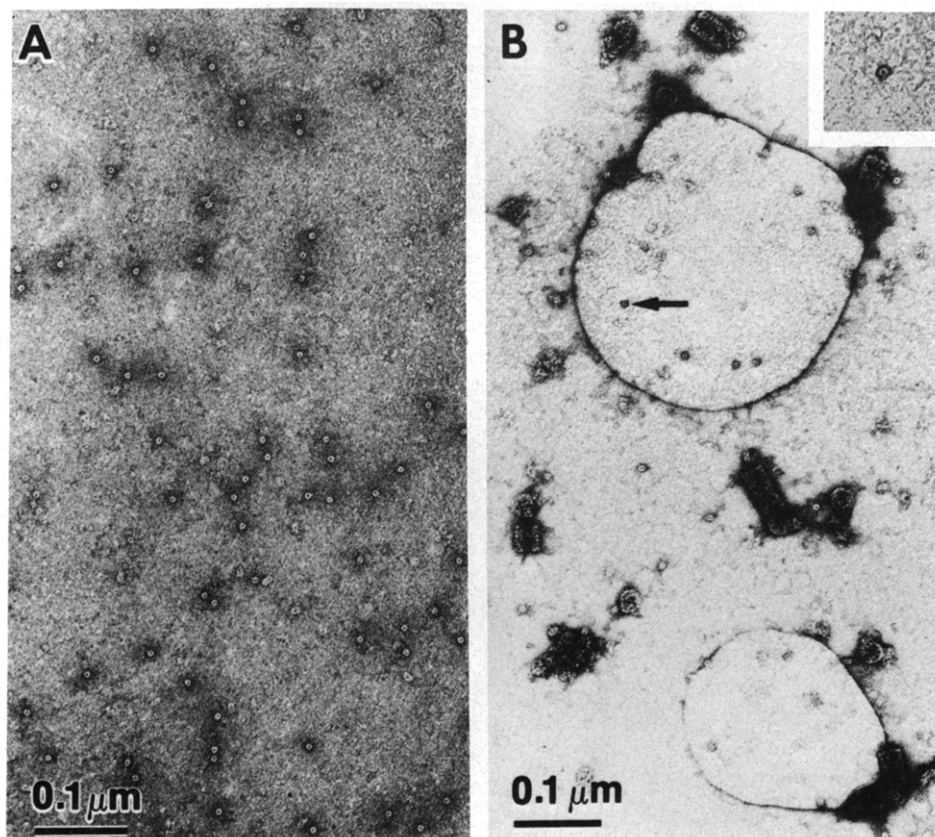


Fig. 2. Electron micrographs of carbon-coated grids which have been cycled through monolayers of fatty acid over a subsolution of keyhole limpet hemocyanin. In A, the field is uniformly covered with lipid and several 70 Å diameter annuli can be seen. The arrows point to three typical annuli. Occasionally, a whole hemocyanin molecule is observed (circle). In B, the transfer of fatty acid to the grid has been less uniform and 'islands' or patches of lipid have been formed. The 70 Å annuli are found attached preferentially to the lipid and the carbon film is nearly devoid of annuli. A higher magnification view of lipid with associated annuli is shown in C.

to be quite distinct both in size and shape from the subunit seen when hemocyanin is dissociated at high pH values [5,8,9]. Occasionally, a whole hemocyanin molecule is seen in the field (circle). Note the relative sizes of the large (300 Å by 300 Å) keyhole limpet hemocyanin molecule and the smaller 70 Å annulus. In certain instances, the transfer of the lipid to the carbon-coated grid is not as uniform and 'islands' or patches of lipid are formed and regions of the carbon-support films are not covered with lipid. In these cases, the 70 Å annuli are found attached preferentially to the lipid patches (Figs. 2B and C) and the carbon film is nearly devoid of annuli. Images of lipid with associated 70 Å annuli are also obtained from grids cycled through monolayers of egg lecithin, dilauroyl lecithin, or bovine brain phosphatidylserine (Fig. 3A). With these phospholipids, the number of annuli observed increases when less volatile alkane solvents, such as decane, are used to form the monolayers. On



**Fig. 3.** Negatively stained preparations of keyhole limpet hemocyanin associated with phosphatidylserine. In A, a carbon-coated grid was dipped through a phosphatidylserine monolayer over a hemocyanin subsolution, while in B phosphatidylserine vesicles were formed in the presence of hemocyanin. The field is relatively uniform in appearance in A and is covered with lipid and 70 Å annuli. Two vesicles with associated annuli are observed in B. There are several hemocyanin molecules and some 70 Å annuli between these vesicles. An enlarged view of an annulus (arrow) in the top vesicle is shown in the insert in B.

the other hand, the 70 Å annuli are not observed when the positively charged lipid, stearylamine, is used.

Control experiments on grids dipped through lipid monolayers over pure water subphases do not show any of the 70 Å annuli. When the keyhole limpet hemocyanin solutions are pretreated to pH values greater than 8.5 and injected

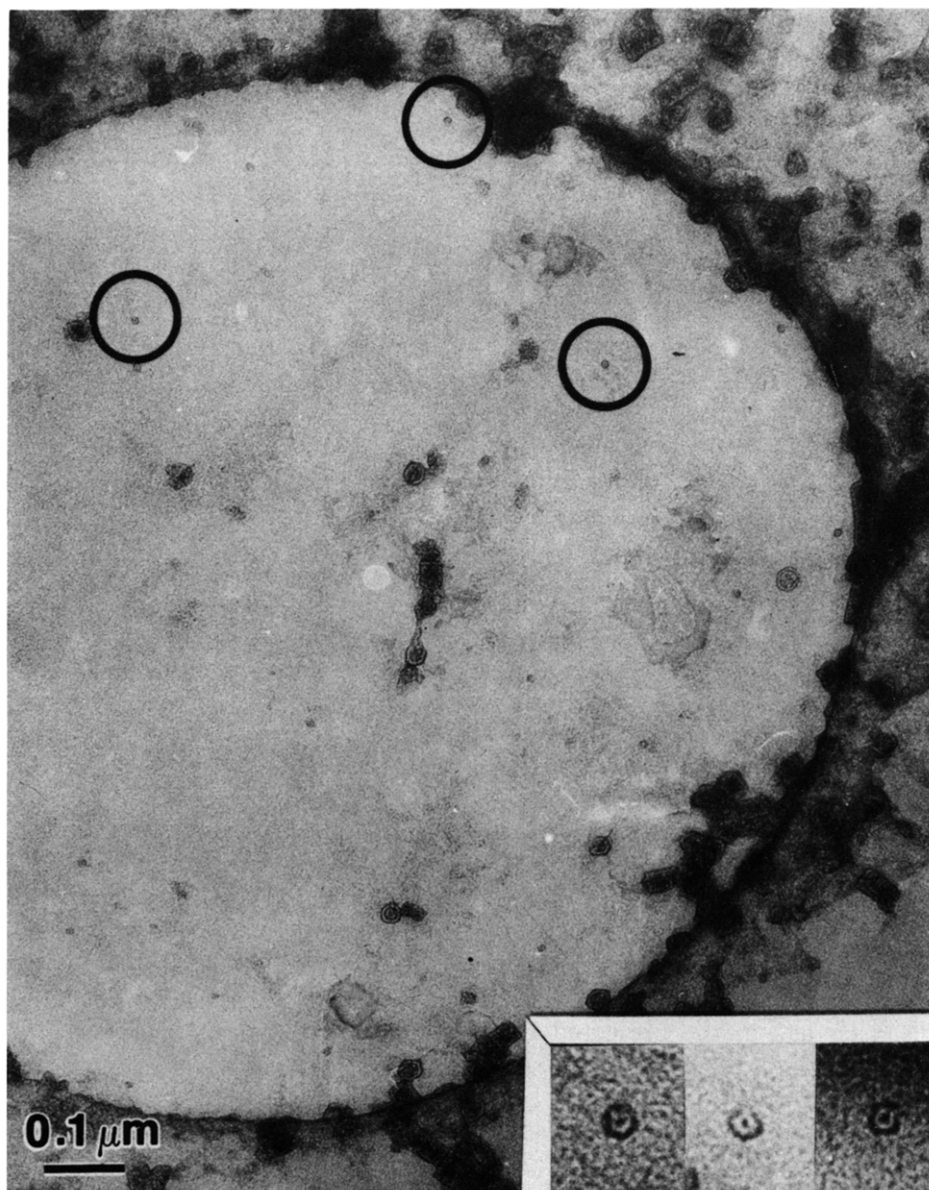


Fig. 4. An image of a 'holey' electron-microscope grid, which was suspended in a keyhole limpet hemocyanin solution, painted with a phosphatidylserine/decane mixture, and negatively stained with uranyl acetate. The large, electron-lucent partial circle which occupies most of the field, is a hole in the grid which is covered by lipid. Several 70 Å annuli can be observed. Three typical annuli are circled and are shown at higher magnification in the insert.



under the monolayer, the dipped grids are covered with the small 30–50 Å subunits of hemocyanin, like those shown in Plate II of van Bruggen and Fernandez-Moran [9].

Fig. 3B is a typical image of bovine brain phosphatidylserine vesicles formed in a keyhole limpet hemocyanin solution. The vesicles display several 70 Å annuli, similar to those seen in Fig. 2. Several hemocyanin molecules, as well as several of the 70 Å annuli, can be seen in the background between vesicles.

Fig. 4 is an image of a holey grid which has been immersed in a keyhole limpet hemocyanin solution and then painted with a phosphatidylserine/decane mixture. This procedure was used to simulate more closely the conditions under which the electrical experiments were performed. The large, light circle which takes up most of this field is a hole in the carbon coat of the grid. The hole is covered by unsupported lipid, as the lipid/alkane mixture which was spread on this grid spontaneously thinned out in the hemocyanin solution so that it appears almost transparent in the electron beam. In many cases, this thin film of lipid and solvent breaks when exposed to the electron beam, and the thinness of the ruptured lipid film can be observed. In this particular instance (Fig. 4), the lipid film remained intact long enough to be imaged. There are several of the 70 Å annuli as well as hemocyanin molecules on the lipid covering the hole, whereas the carbon film at the edge of the hole is covered by complete hemocyanin molecules. The amount of lipid on the carbon-support film is not known. Similar images are seen when bare copper grids are spread with lipid, but they are less stable.

An estimation of the thickness of the negatively stained portion of the 70 Å annulus has been obtained through tilting experiments. Fig. 5 shows images of the same group of particles on a grid which has been tilted 26°. The black bar indicates the orientation of the tilt axis. Fig. 5 shows that the projected appearance of the annuli is only slightly changed when tilted 26°. To quantify the effect of the tilting, we have calculated the ratio  $a : b$  at 0 and 26° tilt, where  $a$  and  $b$  are the respective widths of the annulus in directions perpendicular and parallel to the tilt axis. At 0° tilt, the annuli have an  $a : b$  ratio very close to 1.0, indicating that they are nearly circular. At 26° tilt, the axis parallel to the tilt axis remains the same length, whereas the axis perpendicular to the tilt axis has shortened. In Table I,  $a : b$  ratios for both 0 and 26° tilt angles are presented for 10 different annuli in the field of Fig. 5. The  $a : b$  ratio for these 10 annuli has changed from a mean of  $0.99 \pm 0.01$  at 0° tilt to  $0.87 \pm 0.03$  at 26° tilt. These tilting results provide several pieces of information on the structure of the annulus. Firstly, since there is a change in the projected image, the annulus cannot be spherically shaped. Secondly, since the change in the  $a : b$  ratio is relatively small at a tilt angle of 26°, the annulus must be somewhat wider than it is thick. From these tilting experiments and following the analysis of Zampighi et al. [26], we estimate the negatively stained portion of annulus to be about 25–45 Å thick. If the stained portion of the annulus were much thicker or thinner than this range, the image at 26° tilt would be quite different than at 0° tilt [26]. This 25–45 Å range is a lower limit for the thickness of the entire annulus, since it is possible that a portion of the annulus is not negatively stained. Thirdly, these tilting experiments provide information on the central



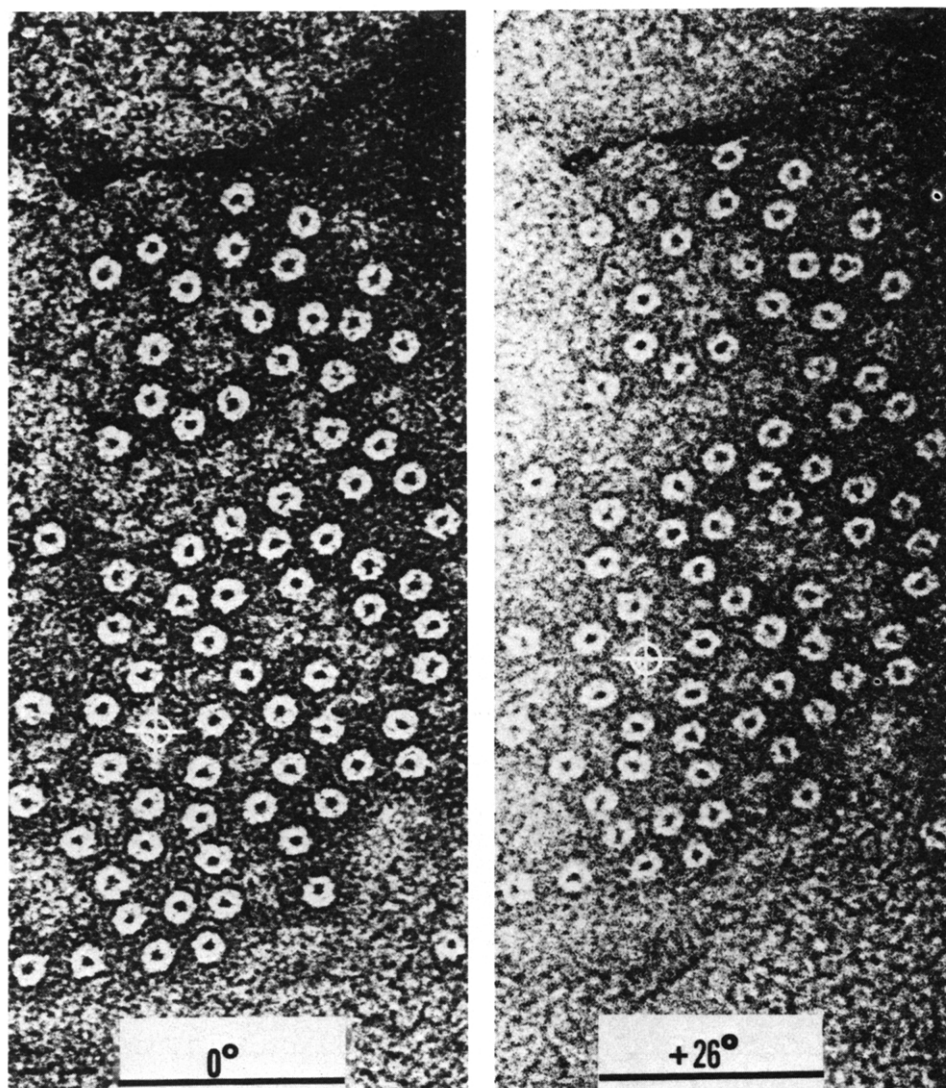


Fig. 5. A fatty acid-keyhole limpet hemocyanin covered grid, similar to the ones shown in Fig. 2, which has been tilted 0 and 26°. The tilt axis is parallel to the black lines at the bottom of the figure. The parameters in Table I were obtained using 10 randomly selected annuli from these images.

pool of stain of the annulus. This central pool does not appreciably change appearance when tilted through 26°. This means that the central pool of stain must be no thicker than the annulus itself and must lie in the same plane as the stain on the outside edge of the annulus.

Both electrical and morphological studies have been performed with other types of hemocyanins and lipid membranes. The hemocyanins from other molluscs such as octopus, whelk and snails do not increase the conductance of black lipid membranes (see Table II). These hemocyanins also have been injected under lipid monolayers. When these monolayers are transferred to

TABLE I

DIMENSIONS  $a$  AND  $b$  OF THE ANNULI IN THE MICROGRAPHS OF FIG. 5 $a$  is the diameter of each annulus perpendicular to the tilt axis and  $b$  is the diameter parallel to the tilt axis.

Annulus number	0° tilt		26° tilt	
	$a$ (Å)	$a:b$	$a$ (Å)	$a:b$
1	75.0	1.00	60.0	0.80
2	78.5	0.96	65.7	0.84
3	72.0	1.00	64.3	0.89
4	75.7	1.00	66.4	0.89
5	71.4	1.01	63.5	0.89
6	72.1	0.97	65.7	0.91
7	72.8	1.00	62.2	0.85
8	75.0	0.99	65.0	0.87
9	71.5	1.00	64.3	0.90
10	70.0	0.98	63.5	0.90
Mean $\pm$ S.D.	73.4 $\pm$ 2.6	0.99 $\pm$ 0.01	64.1 $\pm$ 1.9	0.87 $\pm$ 0.03

TABLE II

EFFECT OF DIFFERENT MOLLUSCAN HEMOCYANINS ON THE MEMBRANE CONDUCTANCE ( $G_m$ ) OF AZOLECTIN BIMOLECULAR LIPID MEMBRANES

Hemocyanin was added to one chamber only. The presence (+) or absence (—) of annuli in negative stain preparations (see text) is given in the last column.

Species	Hemocyanin concentration ( $\mu\text{g/ml}$ )	$G_m$ ( $\Omega^{-1} \cdot \text{cm}^{-2}$ )	70 Å annulus observed
Control	0	$2 \cdot 10^{-8}$	—
<i>Pila</i> (giant snail)	2.4	$3.3 \cdot 10^{-8}$	—
<i>Helix promatia</i> (land snail)	2.0	$3 \cdot 10^{-8}$	—
Octopus	200.0	$4 \cdot 10^{-8}$	—
<i>Busycon</i> (whelk)	300.0	$3.3 \cdot 10^{-8}$	—
Keyhole limpet	1.0	$1.2 \cdot 10^{-6}$	+
	10.0	$4.8 \cdot 10^{-5}$	+

grids and examined with the electron microscope, whole hemocyanin molecules and fragments of hemocyanin molecules are observed with the lipid. However, 70 Å annuli cannot be found.

## Discussion

Speculation on the molecular mechanism of the keyhole limpet hemocyanin-induced ion transport through bilayers has centered on the whole 300 Å hemocyanin molecule or the subunits obtained at high pH values [15, 16]. This paper indicates that there is a third unit which possibly could be the channel former. The 70 Å annulus seen in Figs. 2–5 is different in size and appearance from the whole hemocyanin molecule or the subunit induced by high-pH treatment.

There are several lines of evidence which lead us to believe that the 70 Å annulus could be responsible for the channel formation. First of all, the frequency of observation of these annuli increases tremendously in the presence of lipid. The 70 Å annulus is rarely seen in negative-stain preparations of keyhole limpet hemocyanin solutions, and, indeed, to the best of our knowledge, has never been described in the many previous papers on the structure of molluscan hemocyanins. However, this 70 Å annulus is the predominant proteinaceous unit observed when lipid is present (Figs. 2–5). Whole hemocyanin molecules are sometimes seen with the lipid. However, when the dipped grids are carefully rinsed in water before negative staining, the 70 Å annulus is seen associated with the lipid almost exclusively. Under conditions very similar to those used in the electrical conductance experiments, the 70 Å annulus (along with the whole hemocyanin molecule) is seen associated with the lipid (Fig. 5). Under these conditions, the ratio of 70 Å annulus to whole hemocyanin molecules observed increases as the incubation time of lipid with hemocyanin is increased. Similarly, the membrane conductance increases with time when the bimolecular lipid membranes are exposed to keyhole limpet hemocyanin, indicating that the number of channels increases with time. Secondly, all of the molluscan hemocyanins tested, including keyhole limpet hemocyanin, have similarly shaped molecules and break into subunits at high pH values. However, when the different types of hemocyanin have been exposed to lipids, the 70 Å annulus has only been observed in the case of keyhole limpet hemocyanin. Keyhole limpet hemocyanin is the only one of these hemocyanins tested which produces large conductance increases in black lipid membranes. A third point to be made concerns the relative size of these various proteinaceous units. As Ehrenstein and Lecar [17] have noted, it is difficult to imagine how the large (300 Å by 300 Å) cylindrical keyhole limpet hemocyanin molecule could form a single conducting channel through a thin (approx. 50 Å thick) black lipid membrane. The subunit induced by high pH values [5,8,9] and the 70 Å annulus described in this paper are of a more reasonable size to be considered as single channel formers. However, Blumenthal [15] has shown that the subunits induced by extended dialysis at elevated pH do not form single channels, although they do promote conductance increases. The 70 Å annulus is present under conditions where single channels are formed and it is of a size to be considered reasonably as a channel former. It is also interesting to note that the 70 Å annulus resembles very strongly the nicotinic acetylcholine receptor channel (see Figs. 14 and 15 of Ref. 27) and the 'connexon' of gap junctions [28–31].

Thus, it seems to us that the 70 Å annulus is more likely to be responsible for the formation of single channels than either the whole keyhole limpet hemocyanin molecule or the subunits obtained by pH changes. We cannot, however, rule out the possibility that another hemocyanin unit, unobserved by means of electron microscopy, gives rise to the channel, or that the 70 Å annulus is an intermediate state in the formation of the channel.

Due to the complexity of the hemocyanin molecule [5–7,11], the precise molecular origin of the 70 Å annuli (Figs. 2–5) has not been determined. Since the keyhole limpet hemocyanin as purchased is over 99% pure, it seems likely that the annuli are derived from the hemocyanin molecule rather than

from an impurity in the preparation. There are at least two possibilities to explain why large conductance increases are recorded and the annuli are observed with keyhole limpet hemocyanin and not with the other hemocyanins tested (Table II). First, there may be inherent structural or compositional differences between the various hemocyanin molecules. Second, mild proteolysis may have occurred in the commercially prepared samples, which have been used in our experiments and in the previous electrical conductance experiments [12–14]. Thus, a rearrangement of a partially degraded polypeptide chain might give rise to conductance channels and/or the 70 Å annuli.

The tilting experiments give an estimate of the thickness of the annulus that is embedded in negative stain. They do not provide direct structural information on how deeply the annulus penetrates into the bilayer. In the case of fatty acids (Fig. 5), the tilting experiments show that the thickness of the annulus embedded in negative stain is about 25–45 Å. Since fatty acids are quite impermeable to uranyl acetate [32], this means that the annulus projects into the aqueous phase. Tilting experiments show that the central pool of stain is approximately coplanar with the stain at the outer edge of the annulus, implying that the central pool of stain does not traverse fatty-acid bilayers. However, the annulus may interact differently with planar bimolecular lipid membranes than with vesicles or monolayers. We have not been able to perform tilting experiments on planar lipid/solvent membranes due to the fragile nature of these lipid films on holey grids. Therefore, in the case of these planar membranes, we do not know the position of the central pool of stain relative to the bilayer. We can only say that, in the case of an annulus clearly outlined by negative stain (Fig. 5, insert), some portion of the annulus projects into the aqueous phase. Based on the resemblance of the 70 Å annulus to the connexon of the gap junction [28–31], we speculate that the central pool of stain of the annulus may be related to the conducting channel. However, since the exact three-dimensional shape of this pool of stain has not been determined, its diameter cannot be reliably equated to the width of the channel.

## Acknowledgements

We wish to thank Dr. Ramon Latorre for initially suggesting the studies with hemocyanin and for many helpful comments. We thank Ms. Pat Thompson for an excellent job of typing this manuscript. This work was supported by National Institutes of Health Grant 9 P01 GM 23911.

## References

- 1 Van Bruggen, E.F.J., Wiebenga, E.H. and Gruber, M. (1962) *J. Mol. Biol.* 4, 8–9
- 2 Van Bruggen, E.F.J., Schuiten, V., Wiebenga, E.H. and Gruber, M. (1963) *J. Mol. Biol.* 7, 249–253
- 3 Fernandez-Moran, H., van Bruggen, E.F.J. and Ohtsuki, M. (1966) *J. Mol. Biol.* 16, 191–207
- 4 Mellema, J.A. and Klug, A. (1972) *Nature* 239, 146–150
- 5 Siezen, R.J. and van Bruggen, E.F.J. (1974) *J. Mol. Biol.* 90, 77–89
- 6 Van Bruggen, E.F.J., Schuurhuis, G.J. and van Bruggen, E.F.J. (1977) in *Structure and Function of Haemocyanin* (Bannister, J.V., ed.), pp. 122–127, Springer-Verlag, Berlin
- 7 Gielens, C., Preaux, G. and Lontie, R. (1977) in *Structure and Function of Haemocyanin* (Bannister, J.V., ed.), pp. 85–94, Springer-Verlag, Berlin

- 8 Van Bruggen, E.F.J., Wiebenga, E.H. and Gruber, M. (1962) *J. Mol. Biol.* 4, 1—7
- 9 Van Bruggen, E.F.J. and Fernandez-Moran, H. (1966) *J. Mol. Biol.* 16, 208—211
- 10 Siezen, R.J. and van Driel, R. (1974) *J. Mol. Biol.* 90, 91—102
- 11 Senozan, N.M., Landrum, J., Bonaventura, J. and Bonaventura, C. (1980) in *Structure, Active Site, and Function of Invertebrate Oxygen Binding Protein* (Lamy, J., ed.), Marcel Dekker, Inc., New York, in the press
- 12 Pant, H.C. and Conran, P. (1972) *J. Membrane Biol.* 8, 357—362
- 13 Alvarez, O., Diaz, E. and Latorre, R. (1975) *Biochim. Biophys. Acta* 389, 444—448
- 14 Latorre, R., Alvarez, O., Ehrenstein, G., Espinoza, M. and Reyes, J. (1975) *J. Membrane Biol.* 25, 163—181
- 15 Blumenthal, R. (1975) *Ann. N.Y. Acad. Sci.* 264, 476—482
- 16 Antolini, R. and Menestrina, G. (1979) *FEBS Lett.* 100, 377—381
- 17 Ehrenstein, G. and Lecar, H. (1977) *Q. Rev. Biophys.* 10, 1—34
- 18 Waldbillig, R.C., Robertson, J.D. and McIntosh, T.J. (1976) *Biochim. Biophys. Acta* 448, 1—14
- 19 Harris, W.J. (1962) *Nature* 196, 499—500
- 20 Mueller, P., Rudin, D.O., Tien, H.T. and Wescott, W.C. (1963) *J. Phys. Chem.* 67, 534—535
- 21 Clark, G.L. and Leppla, P.W. (1936) *J. Am. Chem. Soc.* 58, 2199—2201
- 22 Schidlovsky, G. (1965) *Lab. Invest.* 14, 475—495
- 23 Waldbillig, R.C. and Robertson, J.D. (1975) *Biophys. J.* 15, 104a
- 24 McIntosh, T.J., Waldbillig, R.C. and Robertson, J.D. (1976) *Biochim. Biophys. Acta* 448, 15—33
- 25 Clark, G.L., Sterrett, R.R. and Leppla, P.W. (1935) *J. Am. Chem. Soc.* 57, 330—331
- 26 Zampighi, G., Corless, J.M. and Robertson, J.D. (1980) *J. Cell Biol.*, in the press
- 27 Chang, R.S.L., Potter, L.T. and Smith, D.S. (1977) *Tissue Cell* 9, 623—644
- 28 Robertson, J.D. (1963) *J. Cell. Biol.* 19, 201—221
- 29 Goodenough, D.A. (1975) In *Methods in Membrane Biology* (Korn, E.D., ed.), Vol. III, Plenum Publishing Corp., New York
- 30 Zampighi, G. and Unwin, P.N.T. (1979) *J. Mol. Biol.* 135, 451—464
- 31 Unwin, P.N.T. and Zampighi, G. (1980) *Nature* 283, 545—549
- 32 McIntosh, T.J., Waldbillig, R.C. and Robertson, J.D. (1977) *Biochim. Biophys. Acta* 466, 209—230